Original Article
A heptamethine cyanine dye serves as a potential marker for myeloid-derived suppressor cells

Young-Suk Cho[1*], Manh-Hung Do[1*], Hien Duong Thanh[1], Changjong Moon[2], Kwonseop Kim[3], Sang-Hee Cho[4], Hangun Kim[5], Hyung-Ho Ha[5], Chaeyong Jung[1]

[1]Department of Anatomy, Chonnam National University Medical School, Gwangju 61469, Korea; [2]College of Veterinary Medicine, Chonnam National University, Gwangju 61186, Korea; [3]College of Pharmacy, Chonnam National University, Gwangju, Korea; [4]Department of Hemato-Oncology, Chonnam National University Medical School, Gwangju 61469, Korea; [5]College of Pharmacy, Sunchon National University, Sunchon, Jeonnam 57922, Korea. *Equal contributors.

Abstract: Myeloid-derived suppressor cells (MDSCs) are a heterogeneous population of immature myeloid cells with inhibitory effects on T cell-mediated immune response. MDSCs accumulate under many pathological conditions, including cancers, to avoid anticancer immunity. Unlike mouse MDSCs, common specific surface markers for human MDSCs are not clearly defined, mainly due to the complexity of MDSC subsets. In this study, we investigate specific responses of the infrared dye MHI-148 to MDSCs. Mice bearing 4T1 breast cancer cells were established, and splenocytes were isolated. Flow cytometric analyses demonstrated that MHI-148 was reactive to over 80% of MDSC-specific cells manifesting CD11b$^+$/Gr-1$^+$ acquired from both tumor-bearing mice and naive mice. Cells sorted positive for either CD11b/Gr-1 or MHI-148 were also identical to their counterparts (99.7% and 97.7%, respectively). MHI-148, however, was not reactive to lymphocyte or monocyte populations. To determine whether MHI-148-reactive cells exert inhibitory effects on T cell proliferation, an EdU-based T cell assay was performed. MHI-148 reactive cells significantly reduced T cell proliferation with increased arginase activity and nitrite production. In an attempt to test MHI-148 as a marker for human MDSCs, MHI-148 was specifically reactive to CD11b$^+$/CD33$^+$/CD14$^-$ granulocytic MDSCs acquired from selected cancer patients. This study demonstrates that the near-infrared dye MHI-148 specifically reacts to mouse splenocytes with known MDSC-specific markers that have T cell suppressive functions. The dye also selectively binds to a subpopulation of immature myeloid cells acquired from cancer patients. While it is not clear how MHI-148 specifically stains MDSCs, this dye can be a novel tool to detect MDSCs and to predict the prognosis of human cancer patients.

Keywords: Myeloid-derived suppressor cells, MDSC, heptamethine cyanine dye, near infrared dye, MHI-148, IR-783
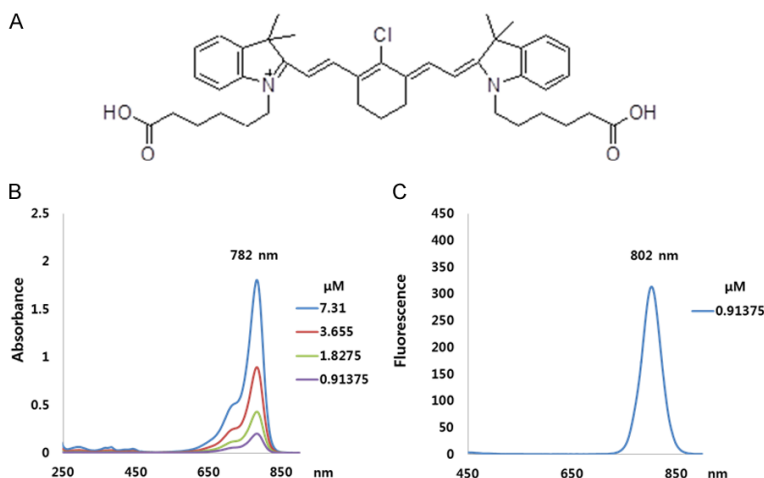
Introduction

Near-infrared (NIR) fluorescence dyes are poly-cyanine heterocyclic compounds that exhibit a emission wavelength between 650-950 nm [1]. NIR dyes are composed of heterocyclic or aromatic rings at both ends or in the middle, and contain intramolecular polymethine chains [2]. Heptamethine cyanine dyes (IR-783 and its derivative MHI-148) have been described as tumor-targeting tools [3]. These dyes are preferentially taken up by tumor cells, and are useful tumor-specific targeting tools in a variety of pre-clinical models [4-9]. Tumor cell-specific uptake

of these dyes were assumed to be due to the differential expression of organic anion-transporting peptides in cancer cells [6, 9]. In addition, there were no systemic toxicity reported by heptamethine cyanine dyes in multiple experimental mouse models [9-12].

Myeloid-derived suppressor cells (MDSCs) are a subset of a heterogeneous population of immature myeloid cells, which function to alter adaptive immunity and induce immunosuppression [13]. These cells are derived from the lineage of dendritic cells (DCs), macrophages, and granulocytes [14]. The population of MDSCs is

Figure 1. Synthesis of MHI-148. Chemical structure of the heptamethine cyanine dye MHI-148 (A). Ultraviolet absorbance (B) and fluorescence (C) of MHI-148.

cell suppression. We also tested the responses of MHI-148 in peripheral blood mononuclear cells (PBMCs) collected from selected cancer patients.

Materials and methods

Synthesis and evaluation of MHI-148

The heptamethine cyanine dye MHI-148 (2-[2-[2-chloro-3-[2-[1,3-dihydro-3,3-dimethyl-1-(5-carboxypentyl)-2H-indol-2-ylidene]-ethylidene]-1-cyclo-hexene-1-yl]-ethyl]-3,3-dimethyl-1-(5-carboxypentyl)-3H-indolium bromide) was synthesized and purified by Bioacts (Incheon, Korea) (**Figure 1A**). Briefly, MHI-148 was purified by HPLC with a retention time of 32 minutes (min). Structural characterization of MHI-148 dye was analyzed by MALDI-TOF-MS. MHI-148 (10 µM) was prepared in 0.1 M PBS buffer (pH 7.45) with 0.25% (v/v) DMSO. The absorption spectra of MHI-148 was measured on a UV-Vis spectrometer (Biomate 5, Thermo Spectronic, Rochester, NY, USA), scanned at a wavelength range of 300-900 nm, and analyzed by VISIONlite (**Figure 1B**). Fluorescence emission spectra were measured with a Horiba FluoroMax 4 spectrofluorometer (HORIBA Jobin Yvon, Edison, NJ, USA). The spectral data were recorded, processed, and plotted using the Origin software (OriginLab, Seoul, Korea) (**Figure 1C**).

Cell line and tumor-bearing mice

The 4T1 mouse mammary carcinoma cell line was purchased from the American Type Culture Collection (ATCC, Manassas, VA, USA). Cells were routinely cultured in DMEM (Invitrogen, Carlsbad, CA, USA) supplemented with 10% FBS and incubated at 37°C in an atmosphere containing 5% CO_2. All cultures were fed with fresh medium every 3-4 days. Female BALB/c mice (7-8 weeks old) were purchased from OrientBio (Seongnam, Korea). All mice were housed under specific pathogen-free conditions in the animal facility at the Hwasun Biomedical Convergence Center. All experiments were performed in accordance with our

maintained at extremely low levels under physiological conditions [14]. However, MDSCs have been found to accumulate under cancerous conditions [14-16]. MDSCs are classified as either polymorphic (granulocytic) MDSCs (PMN-MDSC) or monocytic MDSCs (M-MDSC) [17]. Phenotypes for the two MDSC subtypes in mice have been identified as CD11b^{+} Ly-6C^{low}Ly-6G^{+} for PMN-MDSCs and CD11b^{+}Ly-6C^{high}Ly-6G^{-} for M-MDSCs [18]. Based on these phenotypes, CD11b^{+}Gr-1^{+} is used as a specific marker for MDSCs in mice. Human MDSCs are less well defined. In cancer patients, MDSCs were initially defined as Lin^{-}HLA-DR^{-}CD33^{+} or CD14^{-}CD11b^{+}CD33^{+} cells [19, 20]. PMN-MDSCs are further defined as CD11b^{+}CD14^{-}CD15^{+} (or CD11b^{+}CD14^{-}CD66b^{+}) cells, and M-MDSCs as CD11b^{+}CD14^{+}HLA-DR^{-/low}CD15^{-} cells [21]. CD33 can replace CD11b. However, markers for MDSCs in humans are extremely diverse, and are dependent on the type of cancer or cancer patients [22]. Since the phenotypic heterogeneity of human MDSCs is a big obstacle to understanding their roles in cancer immune systems, exploring specific markers of MDSCs may allow us to characterize and investigate these clinically important cells.

In this study, we demonstrated the possibility of using MHI-148 as a specific marker for MDSCs. We first investigated whether MHI-148 can mimic CD11b^{+}Gr-1^{+} in splenocytes in tumor-bearing mice, followed by determining the characteristic MDSC functions associated with T

institution's guidelines for animal care. The study was approved by the Animal Use and Care Committees at Chonnam National University Medical School. For subcutaneous mammary tumor implantation, mice were injected with 5×10^5 4T1 cells into the flank region. Primary tumors were measured to be 8-10 mm in diameter 21 days after 4T1 cell inoculation.

Reagents and antibodies

Anti-mouse-Gr-1-FITC, anti-mouse-CD11b-PE, purified NA/LE anti-mouse-CD3, and purified NA/LE anti-mouse-CD28 antibodies were purchased from eBioscience (San Diego, CA, USA). Mouse T cell isolation kit, CD8a+ T cell isolation kit, mouse MDSC isolation kit, and MS columns were obtained from Miltenyi Biotec (Auburn, CA, USA). Pepstatin A, aprotinin, antipain, propidium iodide (PI), L-arginine H_2SO_4, α-isonitrosopropiophenone, urea, sulfanilamide, N-1-naphthylethylenediamine dihydrochloride, and sodium nitrite were obtained from Sigma-Aldrich (St. Louis, MO, USA).

Mouse cell isolation and analysis

Spleens of naive or tumor-bearing mice were harvested under sterile conditions. Single-cell suspensions were prepared, and red blood cells (RBC) were removed using the ACK lysing buffer (0.15 M NH_4Cl, 1 mM $KHCO_3$ and 0.1 mM EDTA). Splenocytes (1×10^7) were re-suspended in 1 ml of cold PBS and stained with anti-mouse-Gr-1-FITC and anti-mouse-CD11b-PE antibodies for MDSCs and/or MHI-148 dye (0.5 µM) at 37°C for 30 min. Cells were washed with cold PBS, and then re-suspended in cold Hank's Balanced Salt Solution (2.5% FBS, GIBCO, Carlsbad, CA, USA). Gr-1+/CD11b+ cells and MHI-148-positive cells were analyzed using the FACSCalibur instrument (Becton Dickinson, Heidelberg, Germany). MHI-148-positive cells were isolated using the FACS ARIA II instrument (Becton Dickinson, Heidelberg, Germany). Purity of both Gr-1+/CD11b+ cells and MHI-148-positive cells exceeded 90%. Purification of mouse MDSCs from splenocytes were done using the MDSC isolation kit (Miltenyi Biotech, Auburn, CA, USA), which has been developed for the isolation of Gr-1highLy-6G+ and Gr-1dimLy-6G- myeloid cells according to the manufacturer's protocol. Flow cytometry data were analyzed using either the FlowJo (Becton Dickinson,

Heidelberg, Germany) or Kaluza software (Beckman Coulter, Inc. Brea, CA, USA).

Confocal microscopy

MDSC cells were plated onto 8-well chamber slides under 5% FBS for 16 hours. Cells were briefly rinsed by PBS and fixed with 2% paraformaldehyde at room temperature for 10 minutes. Cells were pre-incubated with 3% normal goat serum followed by incubation with anti-mouse-Gr-1-FITC and anti-mouse-CD11b-PE antibodies (Invitrogen, Carlsbad, CA, USA) with or without MHI-148 (0.5 µM). After washing, slides were covered with anti-fade mounting agent with DAPI and monitored with Zeiss LSM700 confocal microscopy.

EdU-based cell proliferation assays

T cell proliferation assays were performed using a Click-iT EdU assay kit (Invitrogen) according to manufacturer's instructions. Briefly, CD8+ T cells were purified from the spleens of naïve mice via the use of magnetic beads, using the CD8+ T cell isolation kit according to manufacturer's protocol (Miltenyi Biotech, Auburn, CA, USA). Purified CD8+ T cells were cultured in plates coated with anti-CD3 and anti-CD28 antibodies and were maintained in RPMI 1640 containing 10% FBS, 100 U/ml penicillin, 100 mg/ml streptomycin, 50 µM β-mercaptoethanol, and 20 mM HEPES. Purified MHI-148-positive cells or MDSCs were added to the CD8+ T cell-cultured plates, followed by incubation for 2 days. Then, 5'-ethynyl-2'-deoxyuridine (EdU) solution was added at a final concentration of 10 µM, followed by incubation for 2 hrs. Cells were harvested and fixed with 100 µl of 4% formaldehyde at room temperature (RT) for 15 min in the dark. Then, the cells were washed and incubated with 100 µl of saponin-based permeabilization buffer at RT for 15 min. Finally, the cells were incubated with 500 µl of Click-iT reaction cocktail buffer at RT for 30 min and washed with 3 ml of PBS containing 1% BSA. The EdU-stained cells were analyzed using the FACSCalibur instrument. The results of the flow cytometry were analyzed using the Kaluza software.

Arginase activity

Arginase activity was measured in MHI-148 positive cells and MDSCs, as previously described [18]. Cells (1×10^6) were lysed with

100 µl of lysis buffer containing Tris-HCl (pH 7.5), 0.1% Triton X-100, and 100 µg/ml pepstatin A/aprotinin/antipain) at 37°C for 30 min. Subsequently, cell lysates were added into 100 µl 25 mM Tris-HCl (pH 7.5) containing 10 µl of 10 mM $MnCl_2$ and the mixture was heated at 56°C for 10 min. The lysate was further incubated with 100 µl of 0.5 M L-arginine (pH 9.7) at 37°C for 2 hours. The reaction was stopped by adding 900 µl of acid solution mixture (1 H_2SO_4: 3 H_3PO_4: 7 H_2O). Subsequently, 40 µl of 9% α-isonitrosopropiophenone in 100% ethanol was added, and the mixture was heated at 95°C for 30 min. Urea concentration was determined spectrophotometrically by the absorbance of 540 nm measured with a microplate reader. Arginase activities were determined based on the rate of urea production.

Nitric oxide production

Nitric oxide production by MHI-148 positive cells and MDSCs was measured using Griess reagents, as previously described [18]. Briefly, 100 µl of culture supernatant was incubated at RT for 10 min with 50 µl of Griess reagent A (1% sulfanilamide in 2.5% H_3PO_4) and 50 µl of Griess reagent B (0.1% N-1-naphthylethylenediamine dihydrochloride in 2.5% H_3PO_4) in 96-well flat-bottom plates. Nitrite concentrations were determined by comparing the absorbance values of the samples to a standard curve generated by the serial dilution of a solution of sodium nitrite (0.1 mM). Absorbance was measured at 540 nm. Data are representative of three independent experiments.

Human cell isolation and analysis

Heparinized blood samples were obtained from adult patients diagnosed with cancers, prior to the treatment. Blood from healthy donors was also obtained from the Chonnam National University Hwasun Hospital, Korea. All human samples in this study were used according to the Declaration of Helsinki. Written informed consent was obtained prior to obtaining the patient samples. All samples were processed within 12 hours of collection. Whole blood was first treated with the ACK lysing buffer prior to staining, as described above. Next, PBMCs were enriched by density gradient centrifugation using Ficoll-Paque Plus media (GH Healthcare Bio-Sciences, Pittsburgh, PA, USA). Trypan blue was used to determine the viability

of PBMCs prior to flow cytometry analysis. Reactive cell populations were identified by staining cells with fluorophore-conjugated anti-CD11b, anti-CD33, anti-CD14, and anti-CD15 (eBioscience) antibodies for 30 min on ice. The cells were also treated with MHI-148 (in combination). Fluorescence data were acquired using the FACSCalibur instrument. Normalized population statistics, including the median fluorescence intensities (MFIs), were determined using the Kaluza software.

Statistical analysis

Statistical significance between values was determined via Student's t tests. All data were expressed as the means ± standard deviations (SDs). The statistical software SPSS version 21.0 (SPSS Inc., Chicago, IL, USA) was used. Statistical significance was achieved when *p* values were less than 0.05.

Results

MHI-148 is reactive to a fraction of leukemic white blood cells

The near-infrared dyes IR-783 and MHI-148 have shown to be preferentially taken up by tumor cells and tissues [9]. Initially, we tested whether MHI-148 can be used for the detection of leukemic white blood cells. A preliminary study showed that MHI-148 (0.1 µM) was responsive to a small fraction of white blood cells from patients suffering with either chronic myeloid leukemia (CML) or chronic myelomonocytic leukemia (CMML) (**Figure 2A**, **2B**). However, MHI-148 did not respond to white blood cells from patients with acute lymphoid leukemia (ALL) or normal white blood cells (**Figure 2C**, **2D**). In order to identify MHI-148-responsive cells, white blood cells from CML patients were purified and incubated with MHI-148, among which the responding cells were sorted for the live cells (propidium iodide for PE) and MHI-148 for APC (**Figure 3A**). Further cytometric analysis demonstrated that MHI-148-responsive cells were CD11b$^+$/CD33$^+$ cells (**Figure 3B**), suggesting that MHI-148-responsive cells are immature myeloid cells. CD33 is a myeloid marker, and is expressed by myeloid stem cells (CFU-GEMM, CFU-GM, CFU-G, and E-BFU), myeloblasts as well as monoblasts, monocytes/macrophages, granulocytes precursors, and mast cells [23]. CD11b is a
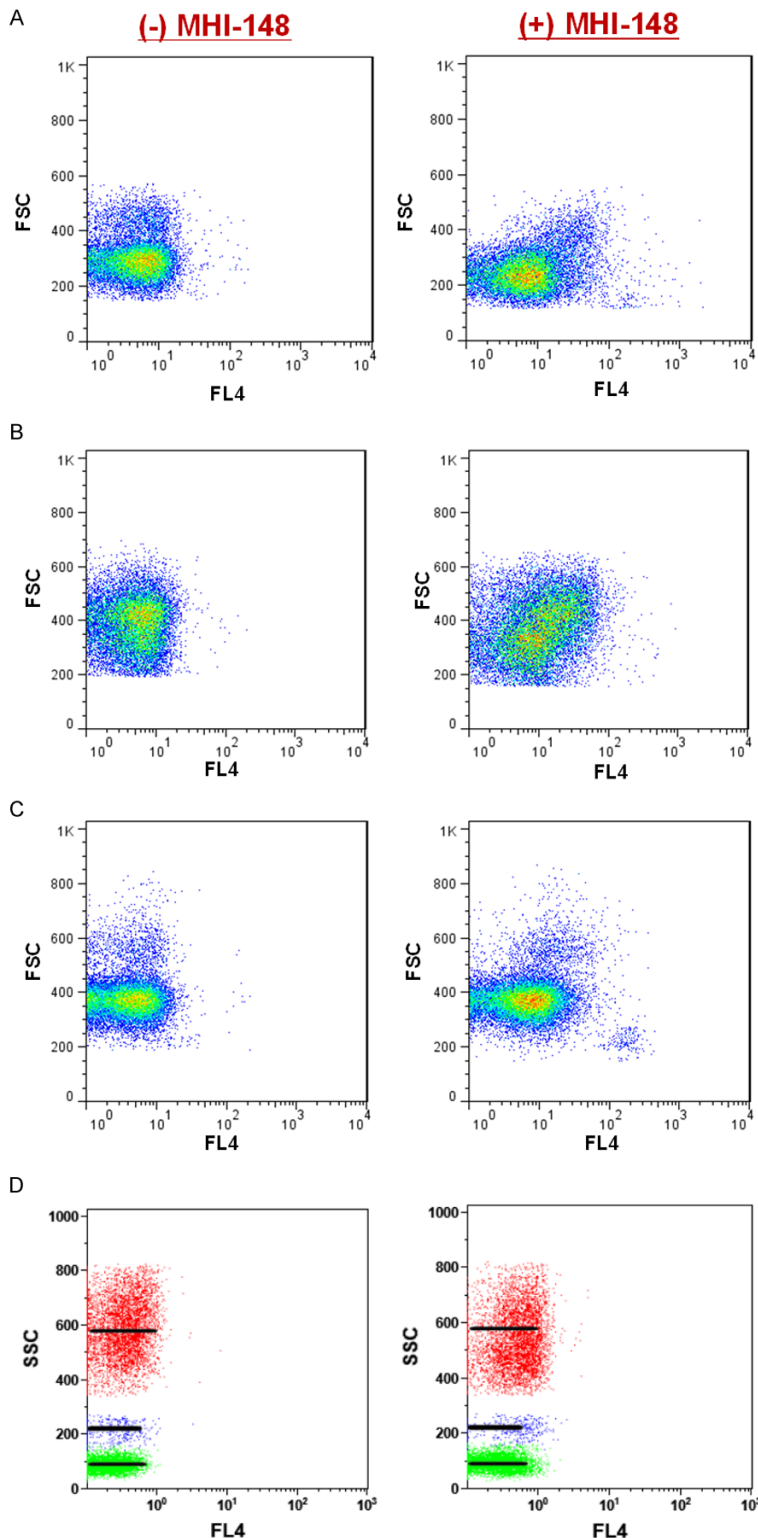
Figure 2. MHI-148 is responsive to the fraction of blood cells from leukemic cancer patients. Peripheral blood was collected in EDTA-coated tubes from patients with chronic myeloid leukemia (A), chronic myelomonocytic leukemia (B), or acute lymphoid leukemia (C). White blood cells from non-cancer patient was also evaluated (D); green, lymphocytes; blue, monocytes; red, granulocytes). RBC-free white blood cells were treated with MHI-148, followed by cytometric analysis using the FACSCalibur instrument. FSC, forward scatter; SSC, side scatter; FL4, MHI-148.

transmembrane glycoprotein for leukocyte adhesion and migration, and can be used as a myeloid marker, similar to CD33 [21]. To further characterize MHI-148-responsive cells, we determined the optimal concentration of MHI-148 using either the granulocytic (middle panel of **Figure 3C**) or lymphocytic (right panel of **Figure 3C**) population of white blood cells from CML patients. A fraction of granulocytes were responsive to MHI-148 in the range of 0.05-5 µM. A fraction of lymphocytes was not responsive to up to 0.5 µM of MHI-148. The optimal concentration of MHI-148 was determined to be 0.5 µM, and this concentration was used for further studies.

MHI-148-responsive cells are Gr-1$^+$/CD11b$^+$ mouse splenocytes

To further clarify the identity of MHI-148-responsive cells, syngeneic BALB/c mice were inoculated with 4T1 breast cancer cells; splenocytes were collected from these mice. RBC-free splenocytes from either tumor-bearing mice or naïve mice were subjected to flow cytometry to observe the cells' responses to MHI-148. Splenocytes were stained with anti-Gr-1-FITC and anti-CD11b-PE antibodies, followed by incubation with MHI-148. Many granulocytes (>80%) from tumor-bearing mice were Gr-1$^+$ and CD11b$^+$. Over 78% of these double positive cells were also reactive to MHI-148 (**Figure 4A**). Splenocytes from naïve mice showed dramatically smaller portion of granulocytes, but most of these cells (>78%) were also Gr-1$^+$/CD11b$^+$/MHI-148$^+$ (**Figure 4B**). As a proof of principle, Gr-1$^+$/CD11b$^+$ cells
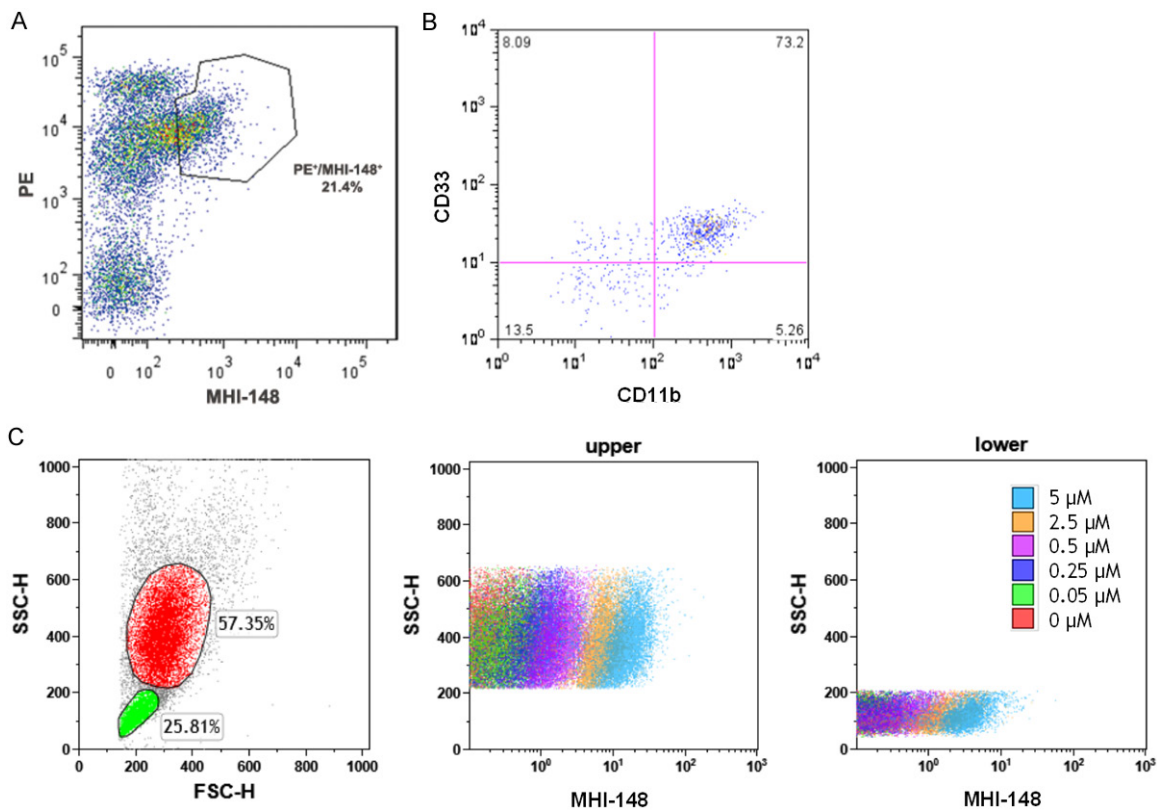
Figure 3. MHI-148-responsive cells are immature myeloid cells. MHI-148-responsive white blood cells from chronic myelomonocytic leukemia (CML) patients were sorted by PE for propidium iodide and APC for MHI-148 (A). Positively sorted cells for MHI-148 were incubated with CD11b and CD33 antibodies and gated (B). Blood cells from CML patients were also incubated with MHI-148 at a final concentration of up to 5 µM and demonstrated by SSC/FSC (C). Response of MHI-148 was shown to either granulocytic fraction (upper) or lymphocytic fraction (lower). Color bars indicate various concentration of MHI-148. FSC, forward scatter; SSC, side scatter; CD, cluster of differentiation.

were purified from splenocytes, and their responsiveness to MHI-148 was observed. Over 99% of Gr-1^{+}/CD11b^{+} cells were reactive to MHI-148 (**Figure 5A**, **5B**). Conversely, MHI-148-responsive cells were isolated using a fluorescence-activated cell sorter. Purified MHI-148-responsive cells were stained with anti-Gr-1 and anti-CD11b antibodies. Over 97% of these MHI-148-responsive cells were reactive to these two markers of mouse MDSCs (**Figure 5C**). These results suggested that MHI-148-responsive mouse splenocytes show phenotypes of Gr-1^{+}CD11b^{+} MDSCs.

MHI-148-reactive cells function as MDSCs

MDSCs exert strong suppressive effects on T cell proliferation. Nitric oxide and arginase are two key molecules that are involved in mediating the immunosuppressive functions of MDSCs [21, 24, 25]. To evaluate whether MHI-148 responsive cells retain their immunosuppres-

sive functions as MDSCs, we first performed T cell proliferation assays. CD8^{+} T cells were purified from the spleens of normal mice and were cultured in anti-CD3 and anti-CD28 antibody-coated plates. Followed by co-culture of either MHI-148 positive cells or MDSCs, CD8^{+} T cells were stained with EdU and analyzed by flow cytometry. Gr-1^{+}/CD11b^{+} cells isolated from 4T1 tumor-bearing mice demonstrated significantly reduced T cell proliferation. Similarly, T cell proliferation was also significantly inhibited by MHI-148^{+} cells (**Figure 6A**). We measured the production of urea to evaluate the arginase activity of MHI-148^{+} cells, along with MDSCs and splenocytes from naive mice. Nitrite production was also measured in these cells using a standard Griess reaction. MHI-148^{+} cells and MDSCs showed markedly higher arginase activity (**Figure 6B**) and nitric oxide production (**Figure 6C**) than those of splenocytes from naive mice. Our findings demonstrated that MHI-148^{+} cells possess immunosuppressive
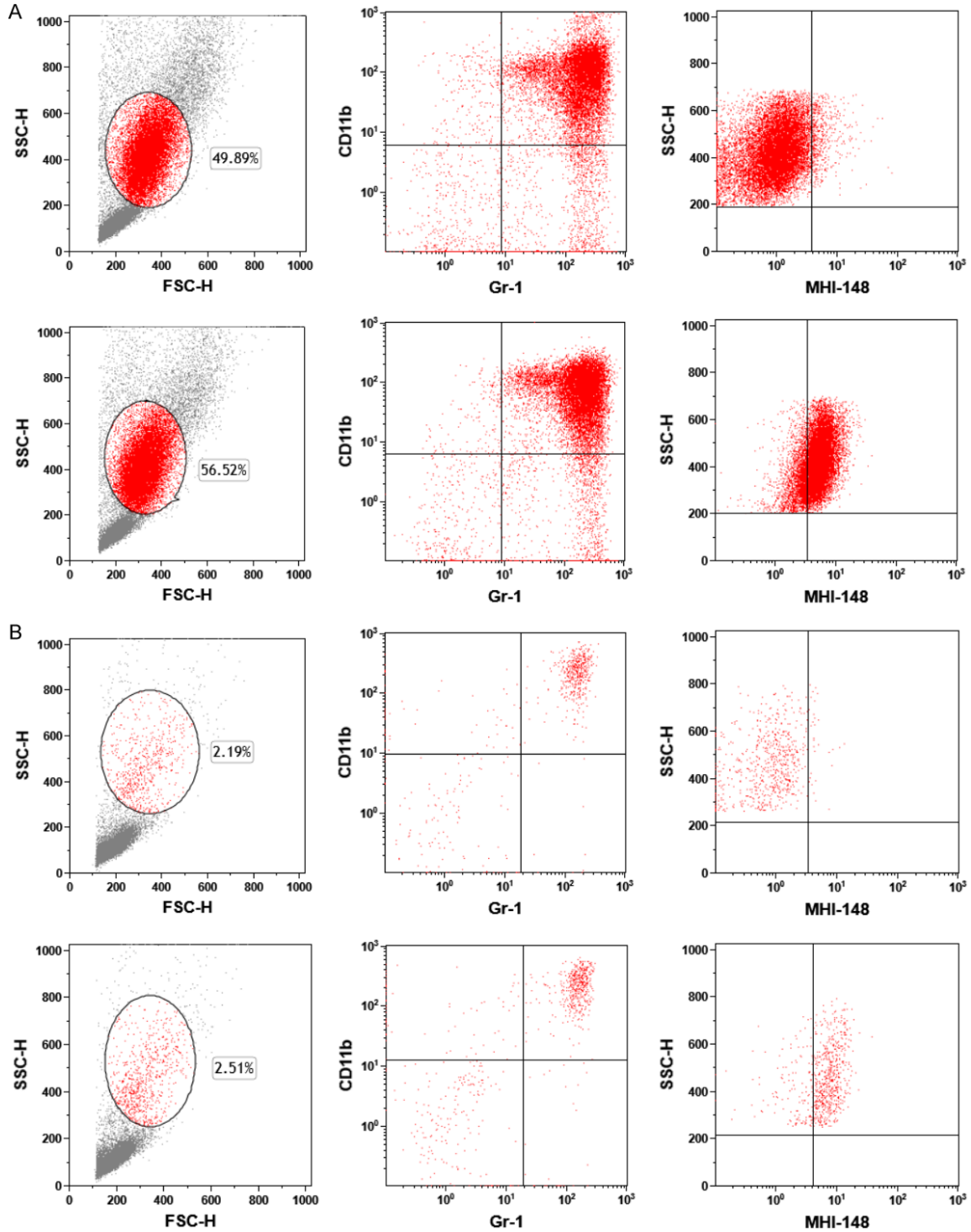
Figure 4. The markers Gr-1 and CD11b are reactive to MHI-148. Splenocytes from 4T1 mammary tumor cells-bearing mice were prepared as described in the Materials and Methods. A population of cells (SSC-H vs. FSC-H) were sub-gated for CD11b and Gr-1, followed by the exclusion of MHI-148-reactive cells. Gr-1$^+$CD11b$^+$ cells were reactive to the MHI-148 dye. Splenocytes were isolated from 4T1-bearing mice at 21 days after injection (A) or from tumor-free mice (B). Cells were stained with anti-Gr-1-FITC, anti-CD11b-PE antibodies in the presence or absence of MHI-148 (0.5 μM). The cells were then washed and analyzed using the FACSCalibur instrument. FSC, forward scatter; SSC, side scatter; CD, cluster of differentiation.
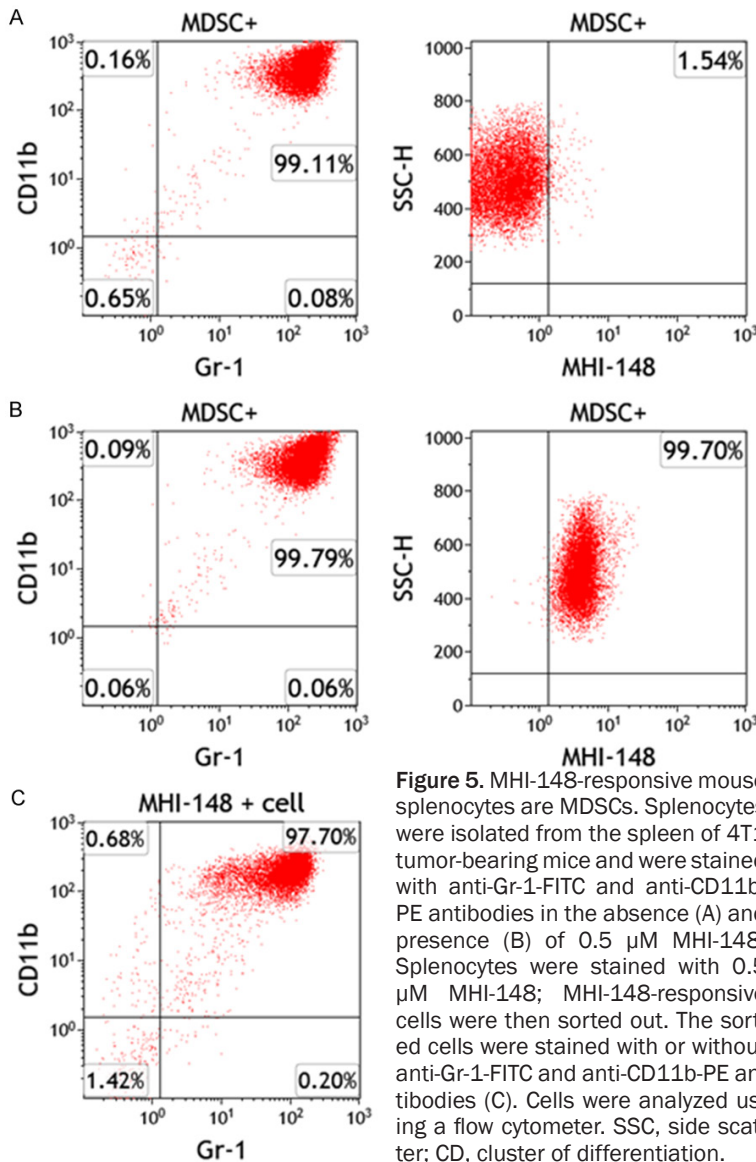
Figure 5. MHI-148-responsive mouse splenocytes are MDSCs. Splenocytes were isolated from the spleen of 4T1 tumor-bearing mice and were stained with anti-Gr-1-FITC and anti-CD11b-PE antibodies in the absence (A) and presence (B) of 0.5 μM MHI-148. Splenocytes were stained with 0.5 μM MHI-148; MHI-148-responsive cells were then sorted out. The sorted cells were stained with or without anti-Gr-1-FITC and anti-CD11b-PE antibodies (C). Cells were analyzed using a flow cytometer. SSC, side scatter; CD, cluster of differentiation.
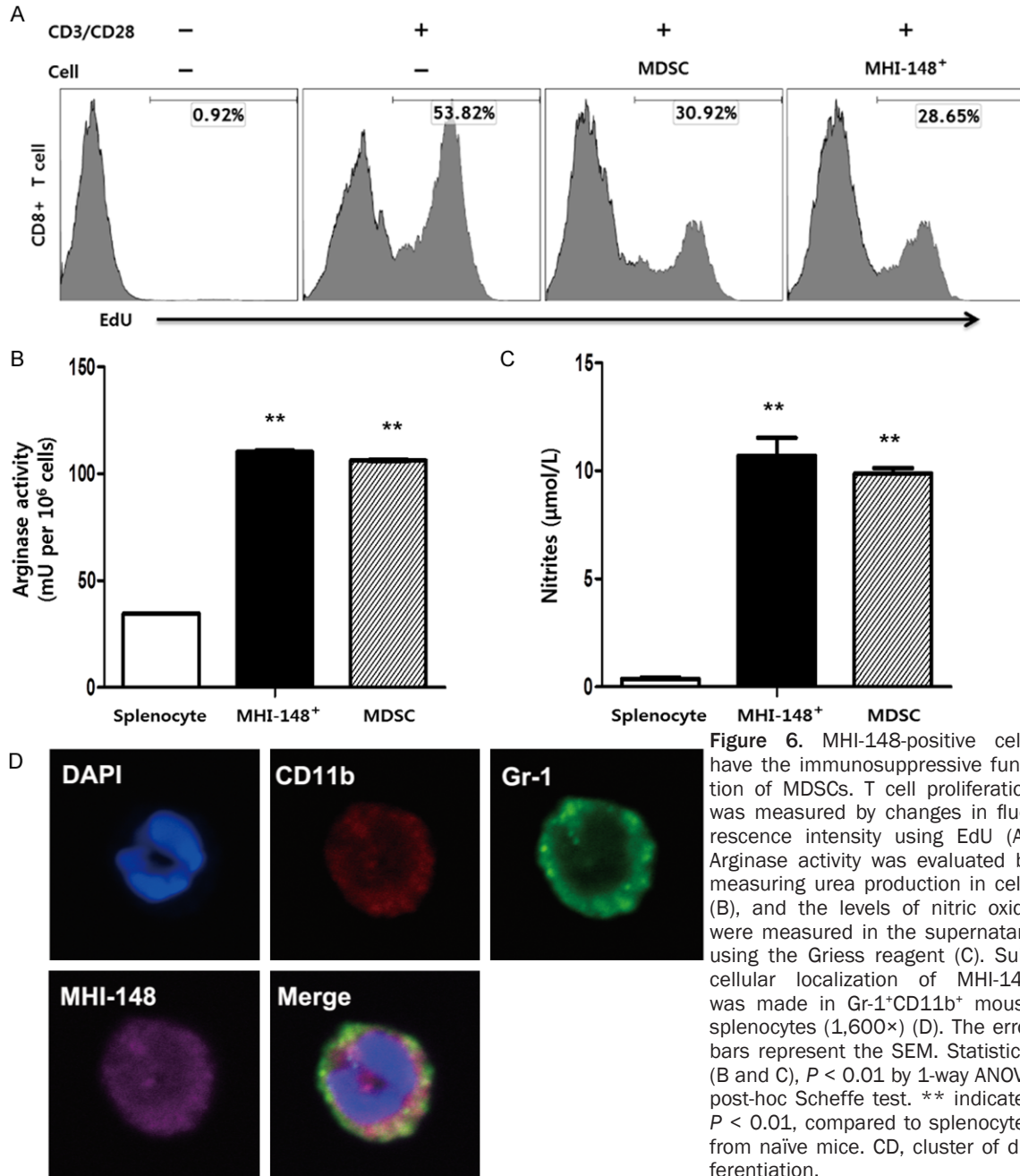
tumor origins were obtained. Using flow cytometry, PBMCs from renal cancer patients were presented as 3 scattered groups: lymphocytes (blue), monocytes (green), and granulocytes (red) (**Figure 7A**). Lymphocytes did not respond to MHI-148 (upper panel of **Figure 7A**). In addition, CD11b$^+$ CD33$^+$ CD14$^-$ granulocytes showed moderate responses to MHI-148 (middle panel), while CD11b$^+$ CD33$^+$ CD14$^+$ monocytes did not show any responses to MHI-148 (lower panel). CD11b$^+$ CD33$^+$ CD14$^-$ granulocytes from cancer patients suffering from various types of cancers showed similar responses to MHI-148 (**Figure 7B**, hepatocellular carcinoma; **Figure 7C**, rectal cancer). Out of the 10 cancer patients' samples, 7 samples showed notable numbers of granulocytic PBMCs, and several of these were MHI-148$^+$ (data not shown). Although more defined studies are needed to clarify similarities between MHI-148-responsive cells and MDSCs via testing for a variety of MDSC phenotypic markers such as HLA-DR, CD15, and CD66b, our study demonstrates that MHI-148 has a specific affinity to the human granulocytic lineage of immature myeloid progenitor cells.

functions of MDSCs, suggesting that MHI-148 specifically stains immunosuppressive MDSCs. We then evaluated cellular distribution of MHI-148. Splenocytes from 4T1 tumor-bearing mice. Mouse MDSCs were isolated by sorting for Gr-1$^+$CD11b$^+$ cells. Confocal analysis of MDSC detected homogenous staining of MHI-148 in both nuclear and cytoplasmic compartments with majority stained in the cytoplasm (**Figure 6D**).

MHI-148 is responsive to human CD11b$^+$/CD33$^+$ PBMCs

To determine whether MHI-148 can be used to detect human MDSCs from cancer patients, blood samples from patients with different

Discussion

Myeloid-derived suppressor cells (MDSCs) are a group of heterogeneous cells that are pathologically differentiated from immature myeloid progenitor cells, including immature DCs, immature macrophages, and immature granulocytes [14, 26, 27]. Myeloid cells normally differentiate from hematopoietic multipotent progenitor cells, resulting in terminally differentiated macrophages, DCs, and granulocytes. These processes are crucial for the normal innate and adaptive immune reactions. Under pathological conditions, however, the tumor
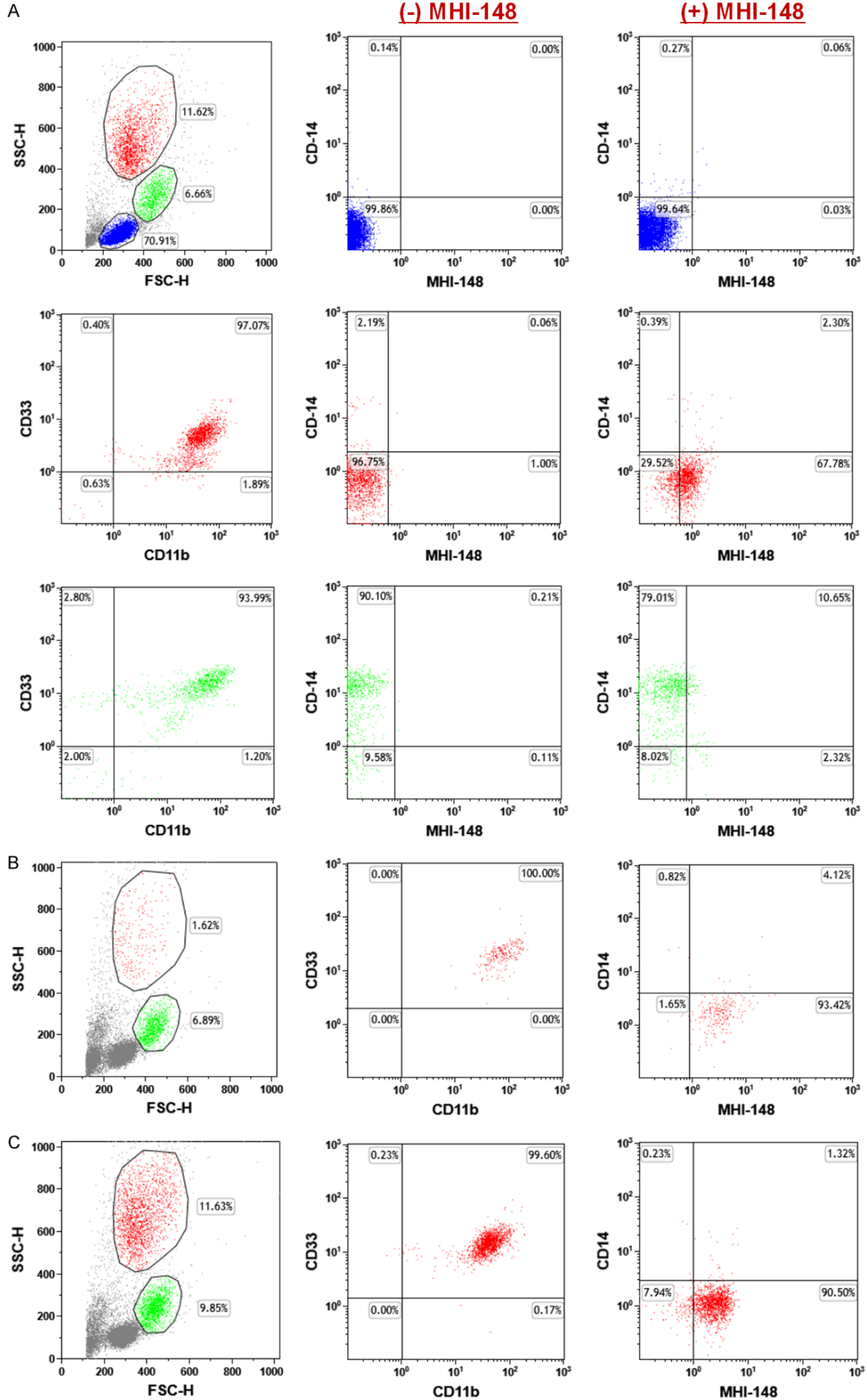
Figure 6. MHI-148-positive cells have the immunosuppressive function of MDSCs. T cell proliferation was measured by changes in fluorescence intensity using EdU (A). Arginase activity was evaluated by measuring urea production in cells (B), and the levels of nitric oxide were measured in the supernatant using the Griess reagent (C). Subcellular localization of MHI-148 was made in Gr-1$^+$CD11b$^+$ mouse splenocytes (1,600×) (D). The error bars represent the SEM. Statistics: (B and C), $P < 0.01$ by 1-way ANOVA post-hoc Scheffe test. ** indicates $P < 0.01$, compared to splenocytes from naïve mice. CD, cluster of differentiation.

microenvironment alters the physiological differentiation process of immature myeloid progenitor cells, resulting in the accumulation of highly immunosuppressive and immature myeloid cells [15, 16]. Therefore, the population of MDSCs is maintained at extremely low levels under physiological conditions, whereas the accumulation of MDSCs has been shown to be promoted in cancers [14]. A major role of MDSCs is the suppression of T cell responses [14]. Several mechanisms by which MDSCs suppress T cell responses have been investigated. One of these mechanisms is the upregulation of arginase 1 (ARG1) and nitric oxide synthase 2 (NOS2) activities by MDSCs [28, 29]. L-arginine (L-Arg) is an essential amino acid for T lymphocyte function; it is converted to urea and L-ornithine by ARG1 or to nitric oxide by NOS2. In addition, MDSCs may also elicit T cell dysfunction via the production of reactive oxygen species [30]. During the process of L-Arg depletion, H_2O_2 is produced, which inhibits the

Near infrared dye to detect MDSCs

Figure 7. MHI-148 cells were CD11b⁺ CD33⁺ CD14⁻ PBMCs from cancer patients. Response of MHI-148 (0.5 μM) to PBMCs from cancer patients was tested. Representative flow cytometry and analysis strategy for PBMCs from renal cancer patients (A). Upper panel, whole cytometric plot demonstrated by SSC/FSC with response of lymphocytic fraction to MHI-148; middle panel, response of granulocytic fraction to MHI-148; lower panel, response of monocytic fraction to MHI-148. Representative flow cytometry and analysis strategy for PBMCs from hepatocellular carcinoma with response of granulocytic fraction to MHI-148 (B). Representative flow cytometry and analysis strategy for PBMCs from rectal cancer with response of granulocytic fraction to MHI-148 (C). lymphocytes (blue); monocytes (red); granulocytes (green); CD, cluster of differentiation; FSC, forward scatter; SSC, side scatter.

expression of T-cell receptors, leading to the G0-G1 phase arrest of T cells.

In this study, we demonstrated that the heptamethine cyanine infrared dye MHI-148 was highly reactive to CD11b⁺Gr-1⁺ splenocytes from tumor-bearing mice. At the same time, MHI-148-responsive cells were found to manifest MDSC-like functions such as suppression of T cell proliferation, stimulation of arginase activity, and increased nitric oxide production. Peripheral blood from cancer patients frequently manifests abnormal accumulation of MDSCs, defined as lymphoid lineage negative, CD11b⁺, HLA-DR⁻/low, and CD33⁺ [31]. These lineage cells are considered to be equivalent to mouse MDSCs [32]. Among these cells, human MDSC were mainly divided two subsets characterized by mutually exclusive co-expression of CD14 or CD15: monocytic (M-MDSCs) as CD14⁺ CD15⁻, and granulocytic (PMN-MDSCs) as CD14⁻ CD15⁺ [32]. A study showed that the CD33⁺ and CD11b⁺ subsets of MDSCs are both HLA-DR^low and lineage⁻ [33]. In these subsets, the expression of the macrophage marker CD68 and the granulocyte marker CD66b was low or absent. Therefore, we simplified our gating criteria using CD33 and CD11b, along with CD14 expression. In PBMCs from selected cancer patients, only CD11b⁺ CD33⁺ CD14⁻ cells were reactive to MHI-148, whereas CD11b⁺ CD33⁺ CD14⁺ cells were not. MHI-148 did not respond to lymphocytes. It is possible that our gating strategy may include unwanted cells and mature neutrophils aside from PMN-MDSCs. Separation of neutrophils from PMN-MDSCs was done using Ficoll-based gradient centrifugation to isolate mononuclear cells. While PMN-MDSCs are enriched in the low-density (mononuclear cell) fraction, neutrophils are high-density cells [34]. Through accidental contamination, the low-density fraction may also contain high-density mature neutrophils in addition to PMN-MDSCs. Therefore, neutrophils may also partly contribute to the fraction of MHI-148-responsive cells isolated from a pool of CD11b⁺ CD33⁺ CD14⁻ cells. To rule out this possibility, more extensive studies are needed to examine specific responses of MHI-148 to various subsets of MDSCs, with the analysis of more comprehensive MDSC phenotype makers, namely, Lin (CD3/14/15/19/56), HLA-DR, CD33, CD11b, CD14, CD15, and CD66b [21, 32]. In addition, tighter control of patients' blood specimens are needed in future studies to avoid contamination from other blood cells. These studies should also include blood from healthy donors as controls. Nevertheless, our study using tumor-bearing mice showed that CD11b⁺/Gr-1⁺ splenocytes, generally considered to be MDSCs, were predominantly MHI-148-positive cells. Since one of our most pressing needs is to identify MDSC markers that would allow the detection of amplified MDSCs from the normal blood cell population in cancer patients, it is worth the challenge to pursue more extensive studies on the MHI-148-specific response of MDSCs from mature myeloid cell populations for future studies.

Despite of NIR dyes having been used as contrast agents in a variety of clinical imaging models [35], their application has been very limited due to their poor stability and lack of targeting specificity [36]. Heptamethine cyanines, including IR-783, MHI-148, and PC-1001, are preferentially accumulated within malignant cells [4, 37, 38]. Subcellular compartments where IR-783 is retained are primarily within the mitochondria and lysosomes, as well as some other cytoplasmic and nuclear compartments [9]. These dyes are thought to be imported into the cells by organic anion transporting polypeptides (OATPs). OATPs are cell membrane-bound transporters involved in the uptake and disposition of a wide array of structurally divergent endogenous and exogenous substrates, including steroid hormones, bile acids, and commonly used drugs [39]. OATPs may play a key role in determining the specific uptake of heptamethine cyanine dyes by cancer cells [9, 40]. The human OATP subfamily OATP5A1 was expressed

in the epithelium of many tissues, including breast cancers, prostate cancers, small cell lung cancers, liver cancers, and colon cancers [41-44]. OATP5A1 is more highly expressed in PBMCs, monocytes, immature dendritic cells, and mature dendritic cells than in macrophages [45]. Furthermore, OATP5A1 expression correlates with the differentiation status of primary blood cells. Therefore, it would be interesting to explore whether MHI-148's responses to MDSCs are attributed to OATPs.

Taken together, this study demonstrated that CD11b$^+$Gr-1$^+$ mouse MDSCs concomitantly respond to the NIR dye MHI-148, which also functions as a T cell growth suppressor. In preliminary studies using human PBMCs from cancer patients, MHI-148 was able to distinguish CD11b$^+$ CD33$^+$ CD14$^-$ cells that were of granulocytic myeloid cell lineages. Considering the complexity associated with the identification of human MDSCs, further studies are required to explore MHI-148 as a useful tool to detect the incumbent amplification of MDSCs in cancer patients.

Acknowledgements

Disclosure of conflict of interest

None.

Address correspondence to: Chaeyong Jung, Department of Anatomy, Chonnam National University Medical School, Gwangju 61469, Korea. E-mail: chjung@jnu.ac.kr

References

[1] Frangioni JV. In vivo near-infrared fluorescence imaging. Curr Opin Chem Biol 2003; 7: 626-634.

[2] Tan X, Luo S, Wang D, Su Y, Cheng T and Shi C. A NIR heptamethine dye with intrinsic cancer targeting, imaging and photosensitizing properties. Biomaterials 2012; 33: 2230-2239.

[3] Yang X, Shao C, Wang R, Chu CY, Hu P, Master V, Osunkoya AO, Kim HL, Zhau HE and Chung LWK. Optical imaging of kidney cancer with novel near infrared heptamethine carbocyanine fluorescent dyes. J Urol 2013; 189: 702-710.

[4] Kushal S, Wang W, Vaikari VP, Kota R, Chen K, Yeh TS, Jhaveri N, Groshen SL, Olenyuk BZ, Chen TC, Hofman FM and Shih JC. Monoamine oxidase A (MAO A) inhibitors decrease glioma progression. Oncotarget 2016; 7: 13842-13853.

[5] Mrdenovic S, Zhang Y, Wang R, Yin L, Chu GC, Yin L, Lewis M, Heffer M, Zhau HE and Chung LWK. Targeting Burkitt lymphoma with a tumor cell-specific heptamethine carbocyanine-cisplatin conjugate. Cancer 2019; 125: 2222-2232.

[6] Shao C, Liao CP, Hu P, Chu CY, Zhang L, Bui MH, Ng CS, Josephson DY, Knudsen B, Tighiouart M, Kim HL, Zhau HE, Chung LW, Wang R and Posadas EM. Detection of live circulating tumor cells by a class of near-infrared heptamethine carbocyanine dyes in patients with localized and metastatic prostate cancer. PLoS One 2014; 9: e88967.

[7] Usama SM, Jiang Z, Pflug K, Sitcheran R and Burgess K. Conjugation of dasatinib with MHI-148 has a significant advantageous effect in viability assays for glioblastoma cells. ChemMedChem 2019; 14: 1575-1579.

[8] Wu JB, Shi C, Chu GC, Xu Q, Zhang Y, Li Q, Yu JS, Zhau HE and Chung LW. Near-infrared fluorescence heptamethine carbocyanine dyes mediate imaging and targeted drug delivery for human brain tumor. Biomaterials 2015; 67: 1-10.

[9] Yang X, Shi C, Tong R, Qian W, Zhau HE, Wang R, Zhu G, Cheng J, Yang VW, Cheng T, Henary M, Strekowski L and Chung LW. Near IR heptamethine cyanine dye-mediated cancer imaging. Clin Cancer Res 2010; 16: 2833-2844.

[10] Lv Q, Yang X, Wang M, Yang J, Qin Z, Kan Q, Zhang H, Wang Y, Wang D and He Z. Mitochondria-targeted prostate cancer therapy using a near-infrared fluorescence dye-monoamine oxidase A inhibitor conjugate. J Control Release 2018; 279: 234-242.

[11] Thavornpradit S, Usama SM, Park GK, Shrestha JP, Nomura S, Baek Y, Choi HS and Burgess K. QuatCy: a heptamethine cyanine modification with improved characteristics. Theranostics 2019; 9: 2856-2867.

[12] Xia X, Gai Y, Feng H, Qin C, Pan D, Song Y, Zhang Y and Lan X. Florescence Imaging Lung Cancer with a Small Molecule MHI-148. J Fluoresc 2020; 30: 1523-1530.

[13] Stewart TJ and Abrams SI. How tumours escape mass destruction. Oncogene 2008; 27: 5894-5903.

[14] Gabrilovich DI and Nagaraj S. Myeloid-derived suppressor cells as regulators of the immune system. Nat Rev Immunol 2009; 9: 162-174.

[15] Marvel D and Gabrilovich DI. Myeloid-derived suppressor cells in the tumor microenvironment: expect the unexpected. J Clin Invest 2015; 125: 3356-3364.

[16] Solito S, Marigo I, Pinton L, Damuzzo V, Mandruzzato S and Bronte V. Myeloid-derived suppressor cell heterogeneity in human cancers. Ann N Y Acad Sci 2014; 1319: 47-65.

[17] Gabrilovich DI. Myeloid-derived suppressor cells. Cancer Immunol Res 2017; 5: 3-8.

[18] Youn JI, Nagaraj S, Collazo M and Gabrilovich DI. Subsets of myeloid-derived suppressor cells in tumor-bearing mice. J Immunol 2008; 181: 5791-5802.

[19] Gabrilovich DI, Velders MP, Sotomayor EM and Kast WM. Mechanism of immune dysfunction in cancer mediated by immature Gr-1+ myeloid cells. J Immunol 2001; 166: 5398-5406.

[20] Ochoa AC, Zea AH, Hernandez C and Rodriguez PC. Arginase, prostaglandins, and myeloid-derived suppressor cells in renal cell carcinoma. Clin Cancer Res 2007; 13: 721s-726s.

[21] Bronte V, Brandau S, Chen SH, Colombo MP, Frey AB, Greten TF, Mandruzzato S, Murray PJ, Ochoa A, Ostrand-Rosenberg S, Rodriguez PC, Sica A, Umansky V, Vonderheide RH and Gabrilovich DI. Recommendations for myeloid-derived suppressor cell nomenclature and characterization standards. Nat Commun 2016; 7: 12150.

[22] Jiang J, Guo W and Liang X. Phenotypes, accumulation, and functions of myeloid-derived suppressor cells and associated treatment strategies in cancer patients. Hum Immunol 2014; 75: 1128-1137.

[23] Garnache-Ottou F, Chaperot L, Biichle S, Ferrand C, Remy-Martin JP, Deconinck E, de Tailly PD, Bulabois B, Poulet J, Kuhlein E, Jacob MC, Salaun V, Arock M, Drenou B, Schillinger F, Seilles E, Tiberghien P, Bensa JC, Plumas J and Saas P. Expression of the myeloid-associated marker CD33 is not an exclusive factor for leukemic plasmacytoid dendritic cells. Blood 2005; 105: 1256-1264.

[24] Kusmartsev S, Nefedova Y, Yoder D and Gabrilovich DI. Antigen-specific inhibition of CD8+ T cell response by immature myeloid cells in cancer is mediated by reactive oxygen species. J Immunol 2004; 172: 989-999.

[25] Zea AH, Rodriguez PC, Atkins MB, Hernandez C, Signoretti S, Zabaleta J, McDermott D, Quiceno D, Youmans A, O'Neill A, Mier J and Ochoa AC. Arginase-producing myeloid suppressor cells in renal cell carcinoma patients: a mechanism of tumor evasion. Cancer Res 2005; 65: 3044-3048.

[26] Talmadge JE and Gabrilovich DI. History of myeloid-derived suppressor cells. Nat Rev Cancer 2013; 13: 739-752.

[27] Veglia F, Perego M and Gabrilovich D. Myeloid-derived suppressor cells coming of age. Nat Immunol 2018; 19: 108-119.

[28] Corzo CA, Condamine T, Lu L, Cotter MJ, Youn JI, Cheng P, Cho HI, Celis E, Quiceno DG, Padhya T, McCaffrey TV, McCaffrey JC and Gabrilovich DI. HIF-1α regulates function and differentiation of myeloid-derived suppressor cells in the tumor microenvironment. J Exp Med 2010; 207: 2439-2453.

[29] Kusmartsev S and Gabrilovich DI. Role of immature myeloid cells in mechanisms of immune evasion in cancer. Cancer Immunol Immunother 2006; 55: 237-245.

[30] Corzo CA, Cotter MJ, Cheng P, Cheng F, Kusmartsev S, Sotomayor E, Padhya T, McCaffrey TV, McCaffrey JC and Gabrilovich DI. Mechanism regulating reactive oxygen species in tumor-induced myeloid-derived suppressor cells. J Immunol 2009; 182: 5693-5701.

[31] Poschke I and Kiessling R. On the armament and appearances of human myeloid-derived suppressor cells. Clin Immunol 2012; 144: 250-268.

[32] Gabrilovich DI, Ostrand-Rosenberg S and Bronte V. Coordinated regulation of myeloid cells by tumours. Nat Rev Immunol 2012; 12: 253-268.

[33] Lechner MG, Megiel C, Russell SM, Bingham B, Arger N, Woo T and Epstein AL. Functional characterization of human Cd33+ and Cd11b+ myeloid-derived suppressor cell subsets induced from peripheral blood mononuclear cells co-cultured with a diverse set of human tumor cell lines. J Transl Med 2011; 9: 90.

[34] Dumitru CA, Moses K, Trellakis S, Lang S and Brandau S. Neutrophils and granulocytic myeloid-derived suppressor cells: immunophenotyping, cell biology and clinical relevance in human oncology. Cancer Immunol Immunother 2012; 61: 1155-1167.

[35] Sevick-Muraca EM. Translation of near-infrared fluorescence imaging technologies: emerging clinical applications. Annu Rev Med 2012; 63: 217-231.

[36] Wu L, Fang S, Shi S, Deng J, Liu B and Cai L. Hybrid polypeptide micelles loading indocyanine green for tumor imaging and photothermal effect study. Biomacromolecules 2013; 14: 3027-3033.

[37] Wu JB, Shao C, Li X, Shi C, Li Q, Hu P, Chen YT, Dou X, Sahu D, Li W, Harada H, Zhang Y, Wang R, Zhau HE and Chung LW. Near-infrared fluorescence imaging of cancer mediated by tumor hypoxia and HIF1α/OATPs signaling axis. Biomaterials 2014; 35: 8175-8185.

[38] Yuan J, Yi X, Yan F, Wang F, Qin W, Wu G, Yang X, Shao C and Chung LW. Near-infrared fluorescence imaging of prostate cancer using heptamethine carbocyanine dyes. Mol Med Rep 2015; 11: 821-828.

[39] Schulte RR and Ho RH. Organic anion transporting polypeptides: emerging roles in cancer pharmacology. Mol Pharmacol 2019; 95: 490-506.

[40] Liu T and Li Q. Organic anion-transporting polypeptides: a novel approach for cancer therapy. J Drug Target 2014; 22: 14-22.

[41] Liedauer R, Svoboda M, Wlcek K, Arrich F, Ja W, Toma C and Thalhammer T. Different expression patterns of organic anion transporting polypeptides in osteosarcomas, bone metastases and aneurysmal bone cysts. Oncol Rep 2009; 22: 1485-1492.

[42] Olszewski-Hamilton U, Svoboda M, Thalhammer T, Buxhofer-Ausch V, Geissler K and Hamilton G. Organic anion transporting polypeptide 5A1 (OATP5A1) in small cell lung cancer (SCLC) cells: possible involvement in chemoresistance to satraplatin. Biomark Cancer 2011; 3: 31-40.

[43] Wlcek K, Svoboda M, Riha J, Zakaria S, Olszewski U, Dvorak Z, Sellner F, Ellinger I, Jager W and Thalhammer T. The analysis of organic anion transporting polypeptide (OATP) mRNA and protein patterns in primary and metastatic liver cancer. Cancer Biol Ther 2011; 11: 801-811.

[44] Wlcek K, Svoboda M, Thalhammer T, Sellner F, Krupitza G and Jaeger W. Altered expression of organic anion transporter polypeptide (OATP) genes in human breast carcinoma. Cancer Biol Ther 2008; 7: 1450-1455.

[45] Sebastian K, Detro-Dassen S, Rinis N, Fahrenkamp D, Müller-Newen G, Merk HF, Schmalzing G, Zwadlo-Klarwasser G and Baron JM. Characterization of SLCO5A1/OATP5A1, a solute carrier transport protein with non-classical function. PLoS One 2013; 8: e83257.